See the related Commentary beginning on page 1235.

Selective parasympathetic innervation of subcutaneous and intra-abdominal fat — functional implications

Felix Kreier,[1,2,3] Eric Fliers,[2] Peter J. Voshol,[3,4] Corbert G. Van Eden,[1] Louis M. Havekes,[4,5] Andries Kalsbeek,[1] Caroline L. Van Heijningen,[1] Arja A. Sluiter,[1] Thomas C. Mettenleiter,[6] Johannes A. Romijn,[3] Hans P. Sauerwein,[2] and Ruud M. Buijs[1]

[1]Netherlands Institute for Brain Research, Amsterdam, The Netherlands
[2]Department of Endocrinology and Metabolism, Academic Medical Center of the University of Amsterdam, Amsterdam, The Netherlands
[3]Department of Endocrinology and Metabolism, Leiden University Medical Center, Leiden, The Netherlands
[4]Netherlands Organization for Applied Scientific Research — Prevention and Health, Gaubius Laboratory, Leiden, The Netherlands
[5]Department of Internal Medicine and Cardiology, Leiden University Medical Center, Leiden, The Netherlands
[6]Institute of Molecular Biology, Friedrich-Loeffler-Institutes, Federal Research Centre for Virus Diseases of Animals, Insel Riems, Germany

The wealth of clinical epidemiological data on the association between intra-abdominal fat accumulation and morbidity sharply contrasts with the paucity of knowledge about the determinants of fat distribution, which cannot be explained merely in terms of humoral factors. If it comes to neuronal control, until now, adipose tissue was reported to be innervated by the sympathetic nervous system only, known for its catabolic effect. We hypothesized the presence of a parasympathetic input stimulating anabolic processes in adipose tissue. Intra-abdominal fat pads in rats were first sympathetically denervated and then injected with the retrograde transneuronal tracer pseudorabies virus (PRV). The resulting labeling of PRV in the vagal motor nuclei of the brain stem reveals that adipose tissue receives vagal input. Next, we assessed the physiological impact of these findings by combining a fat pad–specific vagotomy with a hyperinsulinemic euglycemic clamp and RT-PCR analysis. Insulin-mediated glucose and FFA uptake were reduced by 33% and 36%, respectively, whereas the activity of the catabolic enzyme hormone-sensitive lipase increased by 51%. Moreover, expression of resistin and leptin mRNA decreased, whereas adiponectin mRNA did not change. All these data indicate an anabolic role for the vagal input to adipose tissue. Finally, we demonstrate somatotopy within the central part of the autonomic nervous system, as intra-abdominal and subcutaneous fat pads appeared to be innervated by separate sympathetic and parasympathetic motor neurons. In conclusion, parasympathetic input to adipose tissue clearly modulates its insulin sensitivity and glucose and FFA metabolism in an anabolic way. The implications of these findings for the (patho)physiology of fat distribution are discussed.

This article was published online in advance of the print edition. The date of publication is available from the JCI website, http://www.jci.org. *J. Clin. Invest.* **110**:1243–1250 (2002). doi:10.1172/JCI200215736.

Introduction

The dissimilar distribution of white adipose tissue over the intra-abdominal and subcutaneous fat compartments depends on factors like gender, age, and nutritional condition. Local effects of humoral factors cannot readily explain such distribution, because both compartments are subject to the same endocrine environment, and regional differences in receptor expression are not sufficient to explain the differences (1). Only recently, the biological clock in the hypothalamus was shown to regulate diurnal changes in adipose tissue leptin production (2). This and other evidence indicates that the autonomic nervous system exerts direct control at the cellular and molecular levels in adipose tissue (3). This principle of regulation of adipose tissue is unlikely to be limited to control of leptin secretion only, since the autonomic nervous system plays an important role in the control of energy homeostasis (4–8).

Neuroanatomical and physiological evidence for sympathetic innervation of adipose tissue was presented earlier, suggesting a role for this branch of the autonomic nervous system in lipolysis (9, 10). Parasympa-

Received for publication April 18, 2002, and accepted in revised form August 20, 2002.

Address correspondence to: Felix Kreier, Netherlands Institute for Brain Research, Meibergdreef 33, 1105 AZ, Amsterdam, The Netherlands. Phone: 31-20-566-5500; Fax: 31-20-696-1006. E-mail: f.kreier@nih.knaw.nl.

Conflict of interest: No conflict of interest has been declared.

Nonstandard abbreviations used: pseudorabies virus (PRV); hormone-sensitive lipase (HSL); dorsal motor nucleus of the vagus (DMV); nucleus ambiguus (AMB); green fluorescent protein (GFP); intermediolateral column of the spinal cord (IML); nucleus of the solitary tract (NTS).

thetic innervation, however, was reported to be absent. In the energy-spending, catabolic state of the body, the sympathetic nervous system is predominant (11), whereas in the energy-saving anabolic state, the parasympathetic branch prevails (12, 13). Therefore, we hypothesized the presence of parasympathetic innervation in order to explain the buildup of adipose tissue.

To investigate the innervation of adipose tissue, we used two neuronal retrograde tracers. We injected a retrograde tracer, FluoroGold (Fluorochrome, Englewood, Colorado, USA), and a transsynaptic retrograde tracer, pseudorabies virus (PRV), which is taken up exclusively by neuronal terminals and transported toward the cell body (14–20) into different fat pads in rats. Here, we show that all these fat pads receive parasympathetic input.

In order to asses the physiological impact of the parasympathetic innervation, we applied a hyperinsulinemic euglycemic clamp to determine glucose and FFA uptake in intact as well as in vagotomized retroperitoneal fat pads in the same animal. Sham operated animals were used as a control. Furthermore, we established the activity of hormone-sensitive lipase (HSL), a marker of lipolysis, and the expression of leptin, resistin, and adiponectin mRNA after fat pad–specific vagotomy.

Finally, we hypothesized a selective control of fat compartments by the autonomic nervous system as a neuroanatomical basis for body fat distribution. First, we investigated the organization of parasympathetic motor neurons projecting into the intra-abdominal or subcutaneous compartments. Two retrograde tracers were simultaneously injected into two different fat pads in a single animal: FluoroGold into subcutaneous inguinal fat and PRV into sympathetically denervated retroperitoneal fat. The latter has been reported to be metabolically comparable to omental fat tissue (21). The combination of tracers was used because FluoroGold rapidly and retrogradely fills all neurons that innervate a particular organ, and it is not transported transsynaptically like PRV is. By combining PRV with selective sympathetic denervation, its transport was restricted to the parasympathetic branch of the autonomic nervous system.

Thus, we used neuroanatomical, physiological, and molecular biological methods to elucidate the presence and functionality of parasympathetic input to adipose tissue. Moreover we demonstrated a specialization of autonomic motor neurons projecting into one fat compartment only.

Methods

PRV tracing

Retrograde transneuronal labeling of PRV, a swine neurotrophic α herpes virus, was applied in this study. Uptake, but not replication, by glial cells prevents diffusion of the virus to other neurons (14–20).

Intravenous deposition of 5 μl PRV suspension containing 5×10^6 plaque-forming units [a generous gift of C.E. Jacobs (Institute for Animal Science and Health, Lelystad, The Netherlands)] in the abdominal cavity or on top of a fat pad did not result in labeling of the CNS in six male Wistar rats. Similarly, complete denervation of a fat pad followed by PRV injection in five animals did not result in infection of the CNS. Thus, labeling via blood capillaries in the fat pad did not occur.

Fifteen animals received a single injection of 5 μl of a suspension of the Bartha strain of PRV (PRV-Bartha) containing 5×10^6 plaque-forming units. The injection was performed using a 30-gauge needle connected to a Hamilton syringe at a single spot 1 cm below the most rostral tip of the left retroperitoneal fat pad. By carefully controlling the amount and site of injection, we obtained a reproducible infection rate. In our experience, multiple injections can result in uncontrolled superinfection, probably due to more rapid proliferation of neuronal PRV, resulting in faster lysis of neurons.

Since the level of PRV labeling progresses with time (15), we denote the first neurons in the CNS that were shown to contain PRV as the "first-order neurons." These were all sympathetic and parasympathetic motor neurons. Sacrificing the animals on several time points (3–4 days after injection of PRV), we followed the progress of infection retrogradely from the autonomic motor neurons to the preautonomic neurons (the "second-order neurons") and further upstream. We analyzed five intact animals with first- and second-order infection.

Sympathetic denervation. Twenty-eight animals were used to develop the procedure of sympathetic denervation of the retroperitoneal fat pad. In a series of experiments, we dissected different nerves entering the left retroperitoneal fat pad and then injected PRV. Successful denervation was achieved when the PRV injection resulted in staining of the vagal motor nuclei of the brain stem, but not staining in the spinal cord (see Figure 1). With this approach, the vagal input could be identified and a reproducible denervation technique was developed. The autonomic input to the retroperitoneal fat pad is characterized by diffuse sympathetic nerve fibers, running mostly along blood vessels from the lateral and dorsal directions, and one focused vagal input nerve traveling along blood vessels from the diaphragm into the fat pad.

For histological analysis, sympathetic nerves were removed from a fat pad in 15 animals just prior to PRV injection. The left retroperitoneal fat pad was dissected completely from the connecting tissues except for the nerve bundle traveling along a blood vessel from its rostral tip to the diaphragm. The fat pad was lifted up and inspected for residual nerve bundles. Then PRV was injected in the same way as described above.

Parasympathetic denervation. For the physiological experiments, we reversed the sympathetic denervation procedure. Instead of removing all diffuse input (which has been shown to be sympathetic) and leaving the vagal input along the blood vessel from the rostral tip to the diaphragm intact, we dissected the vagal input only. His-

tological control experiments were conducted to examine the reproducibility of this procedure. We showed in eight of eight animals the absence of any labeling in the vagal motor nuclei after 4 days of survival.

Histological techniques. After 3 days and 4 days, the animals were perfused with saline and then a solution of 4% paraformaldehyde and 0.15% glutaraldehyde in PBS (pH 7.4). They were postfixed overnight and cryoprotected by immersion with 30% sucrose in 0.2 M PBS (pH 7.4) for a further 24 hours. Brain and spinal cord were frozen and coronal sections (40 μm) were cut. After rinsing in 0.05 M Tris-buffered saline (pH 7.4), brain sections were incubated overnight at 4°C with a polyclonal rabbit anti-PRV (anti–α-Aujeszky) antibody (1:10,000; a generous donation of C.E. Jacobs, Institute for Animal Science and Health), then incubated for 60 minutes in the secondary antibody, biotinylated goat anti-rabbit (Vector Laboratories Inc., Burlingame, California, USA), followed by incubation in ABC complex (Vector Laboratories Inc.). Finally, the sections were reacted with 0.025% 3,3-diaminobenzidine tetrahydrochloride in Tris-buffered saline containing 0.5% H_2O_2.

The light microscopy color figures were imported using a Zeiss axioplan 2 microscope (Zeiss, Jena, Germany) fitted with a Progress Camera 3012 (Jenoptik, Jena, Germany). The figures were of 1,488 × 1,120 pixel size in RGB 24-bit true color. Contrast and color were adapted using Adobe Photoshop (Adobe Systems Inc., Mountain View, California, USA) without any other image manipulation.

Glucose and FFA uptake and HSL activity

Animals were either parasympathetically denervated on one side (n = 6, see section on parasympathetic denervation, above) or sham operated (n = 6). Permanent catheters were placed in the jugular vein for infusion and in the inner carotid artery for sampling (22, 23). After 7 days, two pumps were started, one for input of insulin (Actrapid; Novo Nordisk, Chartres, France) at a constant rate of 3.5 mU/kg/min and another for D-glucose (25% solution; Sigma-Aldrich, St. Louis, Missouri, USA). Insulin levels increased to 450 ± 160 versus 533 ± 170 pmol/l, sham versus vagotomy, respectively, while the D-glucose pump was adjusted to maintain blood glucose around 6.0 mM (6.5 ± 1.0 versus 6.6 ± 0.7, sham versus vagotomy, respectively). After glucose reached steady-state levels (~1 hour), a bolus of ^{3}H-2-deoxy-D-glucose (20 μCi; Amersham International, Little Chalfont, United Kingdom) was given to trace tissue-specific glucose uptake. Forty-five minutes later, a bolus of ^{14}C-palmitate (10 μCi; Amersham International) was given to trace tissue-specific FFA uptake. One minute later the animals were killed.

To determine adipose glucose uptake, fat pads were homogenated in water and boiled for 10 minutes. After centrifugation, ^{3}H-2-deoxy-D-glucose-phosphate was separated from free ^{3}H-2-deoxy-D-glucose (present in plasma) by ion-exchange chromatography (Dowex-column X-100; Sigma-Aldrich) to measure tissue glucose uptake. ^{3}H-2-deoxy-D-glucose is taken up by the tissue, converted into ^{3}H-2-deoxy-D-glucose-phosphate, and not metabolized further (24).

Adipose FFA uptake was determined in homogenized fat pads after lipid extraction (25). We confirmed by TLC that no ^{14}C FFAs were incorporated in the lipid fractions (triglycerides and cholesteryl esters).

HSL activity was determined by homogenization of 200 mg of fat pad in buffer containing protease inhibitors (26). The homogenates were centrifuged and the supernatant was used to determine HSL activity with cholesteryl-^{14}C-oleate (Amersham International) as a substrate. All determinations were done in duplicate.

Leptin, resistin, adiponectin, and reference gene mRNA expression

The left retroperitoneal fat pad of nine animals was parasympathetically denervated and was compared

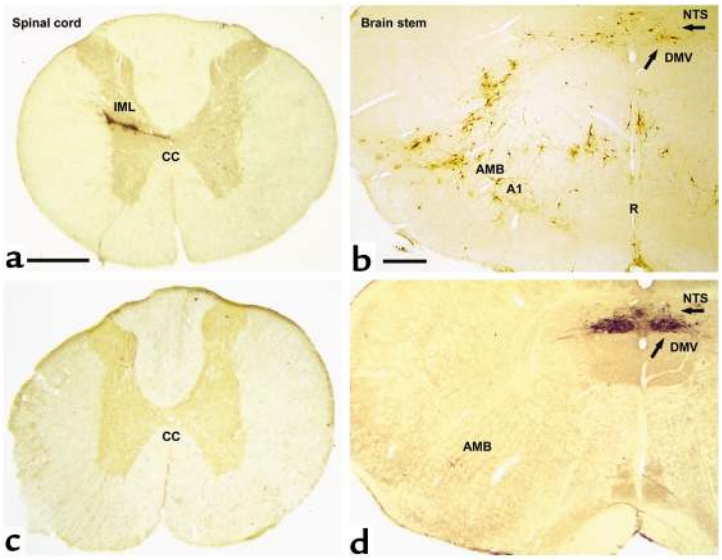

Figure 1
Transverse section of the spinal cord (at Th7) and the rat brain stem at the level of the obex shows spinal cord and brain stem neurons projecting into adipose tissue. Transneuronal retrograde tracing by PRV injection into retroperitoneal fat in rats before (**a** and **b**) and after (**c** and **d**) sympathetic denervation of adipose tissue. In **a** and **b** (PRV tracing from adipose tissue before denervation), since both sympathetic and parasympathetic fibers are intact, PRV is seen to spread via the vagus and the sympathetic nerves. Interestingly, the route via the IML is favored in intact animals such that second-order neurons in the brain stem are already evident when the first-order parasympathetic motor neurons appear in the DMV (arrow). In **b**, the A1 region, the raphe nucleus (R), and the nucleus of the solitary tract (NTS) project into the sympathetic motor neurons. In **c** (with **d**, showing PRV tracing after sympathetic denervation of the left retroperitoneal fat pad), there is no labeling of PRV in the IML. In the brain stem shown in **d**, neurons are clearly visible in the parasympathetic motor nuclei: DMV and caudal part of the AMB. CC, central canal. Bar in **a** and **c** = 0.5 mm. Bar in **b** and **d** = 0.4 mm.

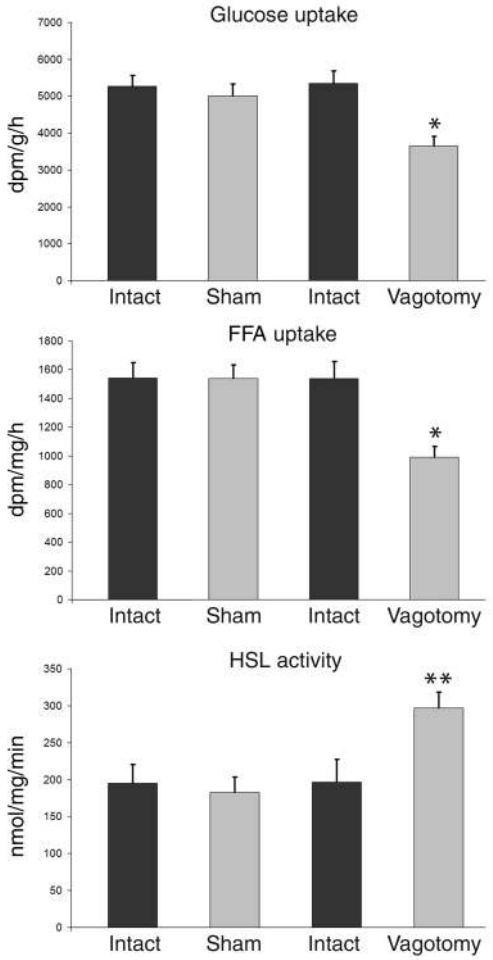

Figure 2
Uptake of glucose and FFA, and HSL activity in adipose tissue after parasympathetic denervation. The left retroperitoneal fat pad was either parasympathetically denervated (n = 6) or sham operated (n = 6). Using a hyperinsulinemic euglycemic clamp, the uptake of ^{3}H-2-deoxy-D-glucose and ^{14}C-palmitate and the activity of the catabolic enzyme HSL were defined. Under these hyperinsulinemic conditions, glucose uptake in the denervated fat pad was reduced by 33% (by Mann-Whitney U test, $*P = 0.02$) and FFA by 36% (Mann-Whitney U test, $*P = 0.02$); HSL activity increased by 51% (Mann-Whitney U test, $**P = 0.03$). Thus, parasympathetic denervation of adipose tissue shifts the metabolism to a catabolic state: uptake of substrate is decreased, while lipolysis increases. Values are expressed as mean ± SEM. dpm, disintegrations per minute.

with the intact right pad. Seven days later, the retroperitoneal fat pads were removed and directly frozen in liquid nitrogen. RNA extraction was performed in Trizol (Life Technologies Inc., Gaithersburg, Maryland, USA) according to the instructions of the manufacturer. Total RNA was reverse transcribed using 2 μg of RNA, 500 ng of oligo-dT, and 200 U reverse transcriptase (SuperScript II RT; Life Technologies Inc.) for 1 hour at 37°C. Quantitative assessment of mRNA levels was performed using a GeneAmp 5700 sequence detection system (PE Biosystems, Foster City, California, USA). RT-PCR was performed using the SYBR Green core reagents kit (PE Biosystems). Primer pairs were designed using Primer Express software (Applied Biosystems, Foster City, California, USA): adiponectin (NM009605), ACAAGGCCGTTCTCTTCACCTA and GGTCCACATTCTTTTCCTGATACTG; leptin (D49653), GGAAGCCTCGCTCTACTCCA and GAATGTCCTGCAGAGAGCCC; and resistin-α (AF323085), GCTCGTGGGACATTCGTGA and CGGGCTGCTGTCCAGTCTA. As a reference, the expression of elongation factor–1α (X63561) was used: AAGCTGGAAGATGGCCCTAAA and AAG-CGACCCAAAGGTGGAT. Amplification efficiency was between 1.98 and 2.07 for the four PCR reactions considered in this study. Sham-operated animals served as control.

Somatotopy: FluoroGold/PRV tracing

Brain stem. Seven animals received a 2-μl injection of 2% FluoroGold solution, a retrograde neuronal tracer, in the left subcutaneous inguinal fat pad. Simultaneously, a 5-μl injection of PRV solution was applied to the sympathetically denervated left retroperitoneal fat pad to show the somatotopic organization of the dorsal motor nucleus of the vagus (DMV). Spinal cord sections were controlled for the absence of PRV as described above. Five animals with only first-order neuronal labeling were included for analysis. In the control group, both tracers were injected into the left sympathetically denervated retroperitoneal fat pad (three of five animals with first-order infection were included for analysis).

Brain stem sections were incubated overnight at 4°C with a polyclonal rabbit anti-FluoroGold antibody (1:15,000; Sigma-Aldrich) and polyclonal mouse anti-PRV (a generous donation of C.E. Jacobs, Institute for Animal Science and Health), and then incubated for 60 minutes with the FITC-conjugated secondary antibody to detect PRV and the CY3-conjugated secondary antibody to detect FluoroGold as described above.

Spinal cord. Sixteen animals received, at the same time, two different strains of PRV: PRV-Bartha β-galactosidase B80 (PRV β-gal) and PRV green fluorescent protein (PRV-GFP). A total of 5×10^{7} plaque-forming units were given of each PRV. PRV β-gal was injected into subcutaneous inguinal fat and PRV-GFP into mesenteric fat without denervation. Animals were sacrificed after 3 days. Both PRV strains showed the same infection rate. As a control, 11 animals (four with first-order labeling included for analysis) received injections of both viruses into the same fat pad.

Sections of thoracic segments of the spinal cord were incubated overnight at 4°C with polyclonal rabbit anti–PRV-GFP (Molecular Probes Inc., Eugene, Oregon, USA) and polyclonal mouse anti–PRV β-gal (Sigma-Aldrich) and then incubated for 60 minutes with the FITC-conjugated secondary antibody to detect PRV β-gal and the CY3-conjugated secondary antibody to detect PRV-GFP.

Results

Parasympathetic innervation of adipose tissue

Neuroanatomy. In the control experiments, intravenous deposition of PRV in the abdominal cavity, on top of a fat pad or into a completely denervated fat pad, never resulted in labeling of the CNS. In contrast, after injection of PRV into the intact retroperitoneal fat pad, the sympathetic preganglionic motor neurons in the intermediolateral column of the spinal cord (IML) were rapidly labeled by PRV. In a later stage of infection (4 days survival), the DMV and nucleus ambiguus (AMB) plus multiple sites in the brain stem and hypothalamus became visible (Figure 1).

Microsurgical denervation of all sympathetic fibers entering the retroperitoneal fat pad combined with injection of PRV selectively infected the antagonistic vagal branch alone without labeling in the spinal cord, where the sympathetic motor nuclei are situated. Six animals were allowed to survive for 3 days and five for 4 days. All animals denervated according to this procedure showed complete sympathetic denervation as evidenced by the absence of sympathetic labeling in the spinal cord. Six animals showed infection beyond the DMV and revealed second-order labeling, while five animals showed first-order labeling only. Among the six animals killed after 3 days, five showed first-order labeling only and one had no staining.

PRV labeling appeared in parasympathetic motor nuclei (DMV and AMB). Subsequently, areas that project into the vagal motor neurons became infected in the brain stem (rostroventrolateral medulla, nucleus of the solitary tract [NTS]), and the hypothalamus (paraventricular nucleus, lateral hypothalamic area).

Physiology. Plasma levels of glucose, insulin, FFAs, cholesterol, glycerol, and triglycerides did not differ between the animals that had the left retroperitoneal fat pad locally vagotomized and the sham-operated animals. Analyzing the ratio between intact and parasympathetically denervated fat pads revealed a 33% (by Mann-Whitney *U* test, $P = 0.02$) reduction in insulin-mediated glucose uptake and a 36% (by Mann-Whitney *U* test, $P = 0.02$) reduction in insulin-mediated FFA uptake in vagotomized fat pads (Figure 2). Interestingly, concurring with the reduced FFA uptake in the vagotomized fat pad, the activity of the catabolic enzyme HSL, the most important enzyme involved in hydrolyzing triglyceride in adipose tissue, increased by 51% (Mann-Whitney *U* test, $P = 0.03$).

Endocrine function. Compared with the intact right retroperitoneal fat pad, resistin and leptin mRNA expression after fat pad–specific vagotomy on the left side decreased by 71% (Mann-Whitney *U* test, $P = 0.001$) and 45% (Mann-Whitney *U* test, $P = 0.004$) respectively, whereas adiponectin and reference gene mRNA did not change significantly (Figure 3). In the control group, mRNA expression of leptin, resistin, adiponectin, and reference gene did not change after sham operations.

Somatotopy

After injection of FluoroGold into the subcutaneous inguinal fat pad and PRV into the sympathetically denervated retroperitoneal fat pad in the same animal, both retrograde tracers were demonstrated within cell bodies of the parasympathetic motor nuclei of the vagus nerve. In all five animals that showed first-order labeling only, the tracers were localized in the same nuclei but in different neurons, which demonstrates a separation of autonomic control at the level of the parasympathetic motor neuron (Figure 4). Vagal motor neurons in the DMV projecting into intra-abdominal fat pads tended to be localized medially to the neurons projecting into subcutaneous fat. As a control, we injected both FluoroGold and PRV into the same sympathetically denervated fat pad. This resulted in colocalization of the tracers, confirming the specificity of the method. Next, the organization of sympathetic motor neurons was investigated by injecting two different strains of PRV: one carrying β-gal into mesenteric fat and the other, with GFP as a marker, into subcutaneous fat. After 3 days, the first neurons appeared in the IML (thoracic segments Th5–Th10). Four animals displaying only first-order labeling of both PRV strains in the sympathetic motor nuclei in the IML were included for analysis. The other animals showed either no infection (two animals), infection with only one PRV strain (eight animals), or a massive infection (two animals). The IML also exhibited staining of the two PRVs, but again in separate neurons (Figure 5). In contrast, if injected into the same fat

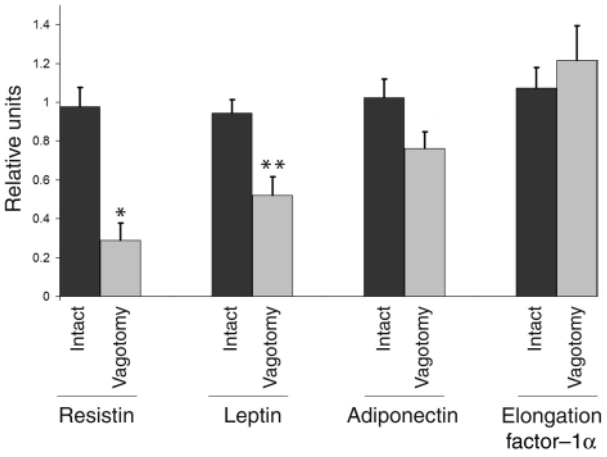

Figure 3
Hormone mRNA expression in adipose tissue after parasympathetic denervation. The left retroperitoneal fat pad was parasympathetically denervated ($n = 9$) and compared with the right intact pad for the expression of mRNA of resistin, leptin, adiponectin, and elongation factor–1α (as a reference gene) by means of real-time RT-PCR. Sham-operated animals were used as control ($n = 5$). While resistin and leptin mRNA expression was reduced (–71%, Mann-Whitney *U* test, $*P = 0.001$; –45%, Mann-Whitney *U* test, $**P = 0.004$, respectively), adiponectin and reference mRNA did not change significantly. Thus, parasympathetic denervation of adipose tissue specifically changes mRNA expression of fat-derived hormones. One relative unit is the equivalent cDNA corresponding with 0.1 μg per well of the pooled cDNA of the control fat pads. Values are expressed as mean ± SEM.

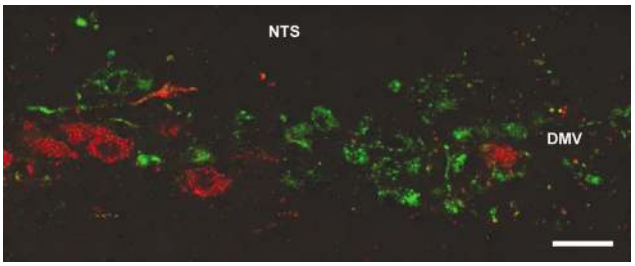

Figure 4
Somatotopic organization of the parasympathetic nervous system. Laser scanning photomicrograph of transverse sections of the brain stem. The central canal is on the right side. Vagal motor neurons project into one fat compartment only (subcutaneous or intra-abdominal). PRV (stained green) was injected into the intra-abdominal fat compartment after sympathetic denervation. At the same time, FluoroGold (stained red) was injected into the subcutaneous fat compartment. Both tracers were transported back to the dorsal motor nucleus DMV and AMB in different neuron populations. Somatotopic segregation can be observed within the DMV. Bar = 50 μm.

pad (mesenteric or subcutaneous inguinal) as a control, both strains of PRV were found in the same neurons.

Discussion

Adipose tissue receives sympathetic and parasympathetic control. PRV injected into the adipose tissue of intact animals resulted in a more rapid labeling of sympathetic motor neurons than occurred in vagal motor neurons. Recent studies have shown that neuronal tracing can be modulated by neuronal activity (27, 28). Also in our study the activity of the vagus nerve modulated the velocity of PRV replication and transport. In the next stage of infection, the transneuronal tracer PRV labeled preautonomic neurons (second order neurons) in brain stem and hypothalamus projecting into the sympathetic motor neurons. In that stage neurons also became visible in the dorsal vagal complex, in which sympathetically-labeled NTS neurons were in proximity to the vagal first-order neurons, making their classification infeasible. This probably explains why parasympathetic innervation of adipose tissue was not noticed in the experiments of Bamshad et al., although their schematic figures showed labeling throughout the dorsal vagal complex (including the DMV) (9).

To distinguish between vagal motor neurons and preautonomic neurons projecting into sympathetic motor neurons, we used two different methods. First, we applied FluoroGold, a nontransneuronal retrograde tracer that reaches the CNS only via preganglionic parasympathetic motor neurons. We found vagal input to various different fat pads (retroperitoneal, mesenteric, epididymal, and subcutaneous inguinal fat). Second, a combination of sympathetic denervation of retroperitoneal fat followed by injection of the transneuronal retrograde tracer PRV prevented infection of the spinal cord, but showed infection of the DMV and AMB. Cutting the readily labeled sympathetic branch forces the virus through the residual branch. As infection continues in an upstream direction, neurons projecting into the vagal motor neurons (i.e., the NTS and rostroventrolateral medulla) become infected. The projection of the same brain areas into vagal motor neurons has been reported earlier from studies of the innervation of the pancreas (20).

At present we cannot answer the question of which transmitters are used by the vagal system to affect adipose tissue. The transmitters used by the vagal system may be (a) acetylcholine, (b) acetylcholine in combination with nitric oxide and/or vasoactive intestinal peptide, or (c) nitric oxide with vasoactive intestinal peptide without acetylcholine (29, 30).

The parasympathetic input to adipose tissue demonstrated in this study illustrates that white adipose tissue receives a dual autonomic control like other (endocrine) organs (4).

Parasympathetic input to adipose tissue modulates insulin-mediated glucose uptake and FFA metabolism in an anabolic way and can selectively modulate its endocrine function. Selective denervation of an intra-abdominal fat pad was chosen instead of subdiaphragmatic vagotomy because the latter changes the neuronal communication between the brain and the whole intra-abdominal compartment (e.g., liver, pancreas, stomach, and intestines). The local vagotomy of one retroperitoneal fat pad allows its comparison with the intact pad on

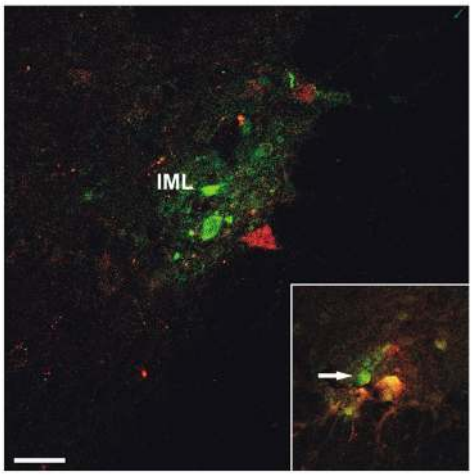

Figure 5
Somatotopic organization of the sympathetic nervous system. Sympathetic motor neurons project into one fat compartment only (subcutaneous or intra-abdominal). Two strains of PRV were injected simultaneously into the intra-abdominal fat compartment (mesenterial fat) and the subcutaneous fat compartment (subcutaneous inguinal fat). Confocal laser scanning photomicrograph of transverse thoracic spinal cord sections (Th5–Th10). Both tracers were transported back to the IML and show clear separation of the different tracers (red/green). Insert (control): Injection of both tracers into the same mesenterial fat pad resulted in colocalization of the two tracers (yellow). Specific laser analysis of the indicated neuron (arrow) also showed colocalization of the tracers with a strong signal of FITC (green) and a much weaker signal of CY3 (red). Bar = 50 μm.

the other side. In addition, because of the surgical complications associated with removing the diffuse sympathetic input, we chose to investigate vagotomy only. Insulin-dependent uptake of glucose and FFAs in adipose tissue was strongly reduced after fat pad–specific vagotomy, while the activity of the catabolic enzyme HSL was increased. The opposite directions of the observed changes indicate that they do not merely reflect a gross change in metabolism or circulation but indeed reflect specific catabolic changes in the adipose tissue after vagotomy. The results show that the anabolic effect of the parasympathetic nervous system on adipose tissue antagonizes the well-known catabolic effect of the sympathetic nervous system (31). Moreover, the endocrine function of adipose tissue is selectively modulated by parasympathetic input. Leptin and resistin mRNA synthesis is decreased in vagotomized fat pads, while adiponectin mRNA synthesis does not change. Thus, the data show a stimulation of the release of resistin and leptin by the vagus nerve (32, 33).

Our results clearly show the physiological impact of parasympathetic innervation on intra-abdominal adipose tissue, indicating its potential to stimulate glucose and FFA uptake, i.e., growth of adipose tissue. The parasympathetic input might mediate in the etiology of obesity by directly influencing the metabolic state of adipose tissue.

Body fat distribution reflects central somatotopic organization. The present study revealed the capacity of the CNS to directly control adipose tissue by means of two different principles: a balance of the sympathetic and parasympathetic output and a selective control of the output with respect to the site of the fat compartment. In other terms, individual central autonomic neurons are specialized to control one fat compartment. Earlier studies of selective peripheral sympathetic control of adipose tissue support our findings (34).

This viscerotopic or rather somatotopic organization reveals the potential of the autonomic motor centers of both branches to selectively affect the anabolism and/or catabolism of either subcutaneous or intra-abdominal fat. Future studies will have to determine whether this somatotopic organization of the autonomic nervous system forms the anatomical basis for the dissociation of intra-abdominal and subcutaneous fat accumulation, i.e., body fat distribution (e.g., in the metabolic syndrome, Cushing syndrome, or AIDS lipodystrophy) (35–40). It is possible that a misbalanced autonomic outflow to the intra-abdominal compartment, including liver, pancreas, and intra-abdominal fat, is an important factor in the pathogenesis of prevalent diseases related to intra-abdominal obesity.

In summary, we show that adipose tissue receives vagal input, modulates its metabolism in an anabolic way, and can selectively stimulate endocrine function. In addition, we demonstrate that parasympathetic innervation differentially modulates the endocrine function of adipose tissue. Finally, we demonstrate a somatotopic organization with respect to the selective innervation of subcutaneous versus intra-abdominal fat by both the sympathetic and parasympathetic nervous systems.

Acknowledgments

We would like to thank Joke Wortel and Marieke Ruiter for technical assistance and Michel Hofman for statistical advice.

1. Wajchenberg, B.L. 2000. Subcutaneous and visceral adipose tissue: their relation to the metabolic syndrome. *Endocr. Rev.* **21**:697–738.
2. Kalsbeek, A., et al. 2001. The suprachiasmatic nucleus generates the diurnal changes in plasma leptin levels. *Endocrinology.* **142**:2677–2685.
3. Ludwig, D.S., et al. 2001. Melanin-concentrating hormone overexpression in transgenic mice leads to obesity and insulin resistance. *J. Clin. Invest.* **107**:379–386.
4. Buijs, R.M., and Kalsbeek, A. 2001. Hypothalamic integration of central and peripheral clocks. *Nat. Rev. Neurosci.* **2**:521–526.
5. Bray, G.A., and York, D.A. 1979. Hypothalamic and genetic obesity in experimental animals: an autonomic and endocrine hypothesis. *Physiol. Rev.* **59**:719–809.
6. Schwartz, M.W., Woods, S.C., Porte, D., Jr., Seeley, R.J., and Baskin, D.G. 2000. Central nervous system control of food intake. *Nature.* **404**:661–671.
7. Ahima, R.S., and Osei, S.Y. 2001. Molecular regulation of eating behavior: new insights and prospects for therapeutic strategies. *Trends Mol. Med.* **7**:205–213.
8. Spiegelman, B.M., and Flier, J.S. 2001. Obesity and the regulation of energy balance. *Cell.* **104**:531–543.
9. Bamshad, M., Aoki, V.T., Adkison, M.G., Warren, W.S., and Bartness, T.J. 1998. Central nervous system origins of the sympathetic nervous system outflow to white adipose tissue. *Am. J. Physiol.* **275**:R291–R299.
10. Penicaud, L., Cousin, B., Leloup, C., Lorsignol, A., and Casteilla, L. 2000. The autonomic nervous system, adipose tissue plasticity, and energy balance. *Nutrition.* **16**:903–908.
11. Scheurink, A.J., and Steffens, A.B. 1990. Central and peripheral control of sympathoadrenal activity and energy metabolism in rats. *Physiol. Behav.* **48**:909–920.
12. Le Magnen, J. 1984. Metabolic and feeding patterns: role of sympathetic and parasympathetic efferent pathways. *J. Auton. Nerv. Syst.* **10**:325–335.
13. Niijima, A. 1989. Nervous regulation of metabolism. *Prog. Neurobiol.* **33**:135–147.
14. Strack, A.M., Sawyer, W.B., Hughes, J.H., Platt, K.B., and Loewy, A.D. 1989. A general pattern of CNS innervation of the sympathetic outflow demonstrated by transneuronal pseudorabies viral infections. *Brain Res.* **491**:156–162.
15. Card, J.P., et al. 1990. Neurotropic properties of pseudorabies virus: uptake and transneuronal passage in the rat central nervous system. *J. Neurosci.* **10**:1974–1994.
16. Card, J.P., et al. 1993. Pseudorabies virus infection of the rat central nervous system: ultrastructural characterization of viral replication, transport, and pathogenesis. *J. Neurosci.* **13**:2515–2539.
17. Loewy, A.D., Franklin, M.F., and Haxhiu, M.A. 1994. CNS monoamine cell groups projecting to pancreatic vagal motor neurons: a transneuronal labeling study using pseudorabies virus. *Brain Res.* **638**:248–260.
18. Jansen, A.S., Nguyen, X.V., Karpitskiy, V., Mettenleiter, T.C., and Loewy, A.D. 1995. Central command neurons of the sympathetic nervous system: basis of the fight-or-flight response. *Science.* **270**:644–646.
19. Billig, I., Foris, J.M., Enquist, L.W., Card, J.P., and Yates, B.J. 2000. Definition of neuronal circuitry controlling the activity of phrenic and abdominal motoneurons in the ferret using recombinant strains of pseudorabies virus. *J. Neurosci.* **20**:7446–7454.
20. Buijs, R.M., Chun, S.J., Niijima, A., Romijn, H.J., and Nagai, K. 2001. Parasympathetic and sympathetic control of the pancreas: a role for the suprachiasmatic nucleus and other hypothalamic centers that are involved in the regulation of food intake. *J. Comp. Neurol.* **431**:405–423.
21. Bjorntorp, P. 1996. The regulation of adipose tissue distribution in humans. *Int. J. Obes. Relat. Metab. Disord.* **20**:291–302.
22. Rossetti, L., Smith, D., Shulman, G.I., Papachristou, D., and DeFronzo, R.A. 1987. Correction of hyperglycemia with phlorizin normalizes tissue sensitivity to insulin in diabetic rats. *J. Clin. Invest.* **79**:1510–1515.
23. Koopmans, S.J., et al. 1991. Whole body and hepatic insulin action in normal, starved, and diabetic rats. *Am. J. Physiol.* **260**:E825–E832.
24. Rossetti, L., and Giaccari, A. 1990. Relative contribution of glycogen synthesis and glycolysis to insulin-mediated glucose uptake. A dose-

response euglycemic clamp study in normal and diabetic rats. *J. Clin. Invest.* **85**:1785–1792.
25. Bligh, E.G., and Dyer, W.J. 1959. A rapid method of total lipid extraction and purification. *Can. J. Biochem. Physiol.* **37**:911–917.
26. Fredrikson, G., Stralfors, P., Nilsson, N.O., and Belfrage, P. 1981. Hormone-sensitive lipase from adipose tissue of rat. *Methods Enzymol.* **71**:636–646.
27. Lee, J.W., and Erskine, M.S. 2000. Pseudorabies virus tracing of neural pathways between the uterine cervix and CNS: effects of survival time, estrogen treatment, rhizotomy, and pelvic nerve transection. *J. Comp. Neurol.* **418**:484–503.
28. Lee, P.G., Cai, F., and Helke, C.J. 2002. Streptozotocin-induced diabetes reduces retrograde axonal transport in the afferent and efferent vagus nerve. *Brain Res.* **941**:127–136.
29. van der Velden, V.H., and Hulsmann, A.R. 1999. Autonomic innervation of human airways: structure, function, and pathophysiology in asthma. *Neuroimmunomodulation.* **6**:145–159.
30. Onuoha, G.N., Alpar, E.K., Chukwulobelu, R., and Nicholls, D.P. 1999. Distributions of VIP, substance P, neurokinin A and neurotensin in rat heart: an immunocytochemical study. *Neuropeptides.* **33**:19–25.
31. Bartness, T.J., and Bamshad, M. 1998. Innervation of mammalian white adipose tissue: implications for the regulation of total body fat. *Am. J. Physiol.* **275**:R1399–R1411.
32. Mueller, W.M., et al. 1998. Evidence that glucose metabolism regulates leptin secretion from cultured rat adipocytes. *Endocrinology.* **139**:551–558.
33. Elmquist, J.K., Elias, C.F., and Saper, C.B. 1999. From lesions to leptin: hypothalamic control of food intake and body weight. *Neuron.* **22**:221–232.
34. Youngstrom, T.G., and Bartness, T.J. 1995. Catecholaminergic innervation of white adipose tissue in Siberian hamsters. *Am. J. Physiol.* **268**:R744–R751.
35. Kissebah, A.H., and Krakower, G.R. 1994. Regional adiposity and morbidity. *Physiol. Rev.* **74**:761–811.
36. Frayn, K.N. 2000. Visceral fat and insulin resistance—causative or correlative? *Br. J. Nutr.* **83**(Suppl. 1):S71–S77.
37. Bjorntorp, P., and Rosmond, R. 1999. Visceral obesity and diabetes. *Drugs.* **58**:13–18; discussion 75–82.
38. Peiris, A.N., et al. 1989. Adiposity, fat distribution, and cardiovascular risk. *Ann. Intern. Med.* **110**:867–872.
39. Despres, J.P., et al. 1990. Regional distribution of body fat, plasma lipoproteins, and cardiovascular disease. *Arteriosclerosis.* **10**:497–511.
40. Reaven, G.M., Lithell, H., and Landsberg, L. 1996. Hypertension and associated metabolic abnormalities—the role of insulin resistance and the sympathoadrenal system. *N. Engl. J. Med.* **334**:374–381.